



HAL
open science

Exploring global accessibility of deep ocean water for sea water air conditioning (SWAC) process: Identifying feasibility areas depending on temperature source

Kanhan Sanjivy, Marania Hopuare, Anthony Jamelot, Franco Ferrucci, Olivier Marc, Franck Lucas

► To cite this version:

Kanhan Sanjivy, Marania Hopuare, Anthony Jamelot, Franco Ferrucci, Olivier Marc, et al.. Exploring global accessibility of deep ocean water for sea water air conditioning (SWAC) process: Identifying feasibility areas depending on temperature source. Sustainable Energy Technologies and Assessments, 2024, 61, 10.1016/j.seta.2023.103601 . hal-04363229

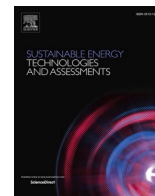
HAL Id: hal-04363229

<https://hal.science/hal-04363229>

Submitted on 24 Dec 2023

HAL is a multi-disciplinary open access archive for the deposit and dissemination of scientific research documents, whether they are published or not. The documents may come from teaching and research institutions in France or abroad, or from public or private research centers.

L'archive ouverte pluridisciplinaire **HAL**, est destinée au dépôt et à la diffusion de documents scientifiques de niveau recherche, publiés ou non, émanant des établissements d'enseignement et de recherche français ou étrangers, des laboratoires publics ou privés.



Exploring global accessibility of deep ocean water for sea water air conditioning (SWAC) process: Identifying feasibility areas depending on temperature source

Kanhan Sanjiv^{a,b,*,1}, Marania Hopuare^a, Anthony Jamelot^c, Franco Ferrucci^a, Olivier Marc^d, Franck Lucas^a

^a GEPASUD, University of French Polynesia, Faa'a, French Polynesia

^b French Environment and Energy Management Agency (ADEME), Angers, France

^c CEA DASE, BP 640, 98713 Papeete, Tahiti, French Polynesia

^d PIMENT, University of Reunion Island, Saint-Pierre, La Réunion, France

ARTICLE INFO

Keywords:

Sea Water Air Conditioning (SWAC)

Deep Ocean Water (DOW)

Resource assessment

ABSTRACT

Sea Water Air Conditioning (SWAC) technology is a highly efficient alternative to conventional air conditioning system using renewable marine energy to provide cooling to buildings. However, its implementation requires access to Deep Ocean Water (DOW) at 4–5 °C, thus SWAC is only viable in coastal regions. Furthermore, one of the major obstacles to its global development is the investment cost that remains high. This cost is strongly linked to the bathymetry of the installation location as it determines the length of the drawing pipeline, which accounts for the largest share of the investment cost. Knowing the temperature and bathymetry profiles will enable the establishment of the financial viability of SWAC technology in a specific location. This paper presents an analysis identifying areas of feasibility on a worldwide scale for standard SWAC implementation first. Then, it explores an alternative design with a higher drawing point for seawater at 12 °C (coupled with a High Temperature District Cooling), which reduces the cost by shortening the drawing pipeline and allows for more locations to be suitable for this technology. Additionally, the impact of the El Niño/Southern Oscillation (ENSO) is also considered since a shallower drawing point makes it more sensitive to temperature variations.

Introduction

Climate change effects already have a noticeable impact on the environment. The risks are multiple, from rising sea levels, to extreme weather events [1]. The increase in cooling needs is, therefore, one of the unavoidable consequences of global warming. The energy consumption induced by building cooling needs has tripled between 1990 and 2016, this tendency is expected to continue until 2050 involving major impact on the electricity system with air conditioning (AC) responsible for ~ 70 % of building's peak power demand [2] in tropical regions. The International Energy Agency (IEA) expects the energy demand induced by AC to multiply by 1.3 for Organization for Economic Co-operation and Development countries and by 4.5 for others [3]. This increase in energy leads to an increase in carbon dioxide emissions, along with the use of refrigerants which are potent greenhouse gases, it

makes the environmental impact of AC significant [4]. This impact can be reduced by improving the Coefficient of Performance (COP) of existing systems and by developing higher-performing alternatives like Sea Water Air Conditioning (SWAC) for coastal areas with access to cold deep ocean water.

The principle of Sea Water Air Conditioning (SWAC) is quite straightforward: Deep Ocean Water (DOW) is drawn through a pipeline, and its cooling energy is transferred to a District Cooling (DC) through heat exchangers. The warmed-up seawater is released back into the shallow sea. Fluids in the installation are moved by circulator pumps.

For the classic operating process of SWAC system, seawater at approximately 4 to 5 °C is drawn from a depth of 960 m in the ocean and discharged at –30 m. It enters the heat exchanger at 6 °C and leaves at 11 °C. The District Cooling system generally operates with a 7/12 °C temperature regime. The characteristics of SWAC technology makes it particularly suitable for insular territories that have a favorable

* Corresponding author at: French Environment and Energy Management Agency (ADEME), Angers, France.

E-mail address: kanhan.sanjiv@doctorant.upf.pf (K. Sanjiv).

¹ 20, avenue du Grésillé- BP 90406 49004, Angers Cedex 01, France

Nomenclature

| | |
|----------------------------|---------------------------------------------------------------------------|
| AC | Air Conditioning |
| ASHRAE | American Society of Heating, Refrigerating and Air-Conditioning Engineers |
| COP | Coefficient of Performance |
| DC | District Cooling |
| DOW | Deep Ocean Water |
| ENSO | El Niño/Southern Oscillation |
| GEBCO | General Bathymetric Chart of the Oceans |
| GLORYS | Global Ocean Physics Reanalysis |
| HTDC | High Temperature District Cooling |
| ORC | Organic Rankine Cycle |
| OTEC | Ocean Thermal Energy Conversion |
| SWAC | Sea Water Air Conditioning |
| TC; PC; FC | Total Cost; Pipeline Cost; Fixed Cost |
| T_{sw} | Seawater temperature source |
| UTCI | Universal Thermal Climate Index |

bathymetry, that is, with great depths near the coast. That is the case for French Polynesia which has three SWAC installations operating for cooling production in real conditions.

According to the energy performance assessment of Tetiaroa installation [5], the SWAC's global Coefficient of Performance (COP), which includes the electricity consumption of the district cooling system, is in the 15–20 range. This makes the technology a highly efficient alternative to conventional air conditioning systems, considering that the COP of a large split system doesn't exceed 5 [2]. The primary circuit of SWAC can also be compared to other traditional centralized systems. For instance, while the best COP available for chillers is around 12 [2], the COP of the SWAC primary circuit can reach approximately 140 to 150 [5].

The three SWAC installations in French Polynesia are for air conditioning purpose only and they operate with the regular settings presented above. Two installations with a similar principle to SWAC using a lake (deep lake water cooling) exist in Canada and the Netherlands, despite much lower air conditioning requirements than in tropical climates [6]. Other related systems exist in France, like the "Fraîcheur de Paris" system [7] which draws chilled water from the river Seine in Paris, and the marine geothermal plant Thassalia producing both heat and cold in Marseille [8]. The temperature difference between deep and shallow seawater can also be utilized to produce electricity through a thermodynamic cycle, such as the Organic Rankine Cycle (ORC). In this type of installation, called Ocean Thermal Energy Conversion (OTEC), the warm surface ocean water serves as the hot source, while the deep ocean water acts as the cold source [9]. Currently, three installations of this type are operational. They are located in Hawaii [10,11], Japan [12,13], and South Korea [14,15], with electric powers of 100 kW for the first two and 20 kW for the third one.

While the investment cost of this technology is very high, it remains interesting in French Polynesia due to the high cost of electricity caused by insularity and the significant cooling needs of the tropical climate. The major cost of an SWAC installation is due to the drawing pipeline, which can get unreasonably expensive depending on the bathymetry down to the 5 °C isotherm. This strong link between bathymetry and cost of SWAC systems is one of the reasons why this technology remains scarce outside of French Polynesia. The 5 °C drawing point was initially selected to match the common temperature regime of District Cooling, which is 7 °C inlet and 12 °C outlet. However, this standard regime is not necessarily well adapted for deep-water-based cooling systems given the zone temperature required for thermal comfort.

Guidelines for thermal comfort in buildings are provided by the American Society of Heating, Refrigerating and Air-Conditioning

Engineers (ASHRAE), which aim to satisfy the vast majority of building occupants. These guidelines recommend a temperature between 20 °C and 23 °C during winter and between 22 °C and 27 °C for summer. The relative humidity inside the building should be between 30 % and 60 % [16]. According to these recommendations, air conditioning system in tropical climate shall generally target an interior temperature of 26 °C with a relative humidity of 60 % in order to limit energy consumption while ensuring thermal comfort.

Framed within this context, this work analyzes the possibility of raising the drawing point up to 12 °C and adjusting the temperature range of the District Cooling to a 14/22 °C regime, also known as High Temperature District Cooling (HTDC) [17]. This alternative could be a solution to greatly reduce the cost of SWAC installation by shortening the drawing pipeline to a reasonable length, while also expanding the application of SWAC technology to previously unsuitable locations. Both objectives contribute to a greater adoption of the technology worldwide. The increase in the temperature of the district cooling loop must nevertheless allow the dehumidification of the fresh air in order to maintain an acceptable indoor relative humidity, in particular for tropical climates. Note that a 14/22 °C regime can very often ensure dehumidification when necessary. Indeed, for example, for the climate of Polynesia, the outdoor air dewpoint temperature is higher than 22 °C more than 78 % of the time, thus allowing the condensation of water vapor. If necessary, additional dehumidification of the fresh air could be ensured by an additional desiccant device.

Currently, the majority of designers set the chilled water temperature regime at 7/12 °C. Embracing an energy efficiency approach, the building's air temperature is set at a minimum of 26 °C and can go up to 28 °C by using a ceiling fan [18]. It appears interesting to reconsider this 7/12 °C chilled water temperature regime and increase it: For conventional mechanical vapor compression chillers, raising the chilled water temperature regime would lead to energy savings, as the chiller would be more efficient with a higher evaporation temperature, reducing thermal losses. A preliminary study in temperate climates estimated a 26 % reduction in electrical consumption for a conventional system operating on the 12 °C/16 °C regime compared to the 6 °C/12 °C regime [19]. For Sea Water Air Conditioning (SWAC), this increase would significantly reduce both investment and operating costs since the length of the seawater pipeline would decrease significantly. It would also extend SWAC applications to regions where water depths were not conducive to producing chilled water at 7 °C. However, when increasing chilled water temperatures, the dehumidification of the building's air becomes less effective. Therefore, it is necessary to find an optimum balance between the chilled water regime and the building's comfort conditions. This issue is even more critical in humid tropical regions such as Tahiti or La Réunion. In 2008, the PIMENT laboratory installed a solar absorption cooling system capable of cooling multiple classrooms at the University of La Réunion [20,21]. The sizing of this installation is based on a chilled water regime of 11 °C/17 °C (corresponding to an average cold battery temperature of 14 °C) and allows cooling the rooms to a minimum temperature of 24 °C at 60 % relative humidity. Therefore, with the 11/17 °C regime, this installation easily achieves air temperature setpoints between 26 °C and 28 °C.

However, raising the drawing point could result in seasonal or inter-annual temperature variation, including phenomena like El Niño/Southern Oscillation (ENSO) [22–25]. For this reason, the impact of ENSO will be taken into account in this work for this raised drawing point. An assessment of the technical potential of SWAC with cost estimates was already made by Hunt [26]. Data on ocean temperature, bathymetry and surface air temperature were analyzed on a global scale. The study estimated the pipeline length required to access seawater at 5 °C or lower from the coastline. This estimation was combined with a projected demand for air conditioning, considering a predefined SWAC design for air cooling from 30 °C to 20 °C. The resulting pipeline length and capacity factor were then used to approximate costs associated with SWAC projects worldwide. The study concluded that there is a high

potential for SWAC implementation in intertropical islands like the Caribbean, and some continental locations like the west coast of Mexico, Colombia, and northeast of Brazil.

This study introduces various innovations. Firstly, it explores the potential of an alternative SWAC design with a targeted drawing temperature of 12 °C, comparing it to the traditional design which uses a 5 °C temperature source. The seawater temperature dataset is also enhanced, offering a higher precision of 1/12° resolution, in contrast to the previous 1° resolution. This enhanced precision is crucial for accurately calculating changes in the drawing point temperature. Considering the technical limitations encountered in the Tahiti SWAC project, a maximum viable distance of 15 km is set. This distance constraint provides a more realistic estimation of SWAC potential. Moreover, instead of solely relying on ambient air temperature, the study employs the thermal comfort index to identify suitable areas for SWAC implementation based on air conditioning requirements. Finally, the cost data used in this study are derived from the actual expenses of the last SWAC installation in Tahiti, rather than relying on cost estimates from a pre-feasibility study, as seen in the existing state of the art.

Data and methods

Input datasets: Bathymetry; seawater temperatures and thermal climate index

In this study, the three following datasets will be used to identify SWAC feasibility areas: General Bathymetric Chart of the Oceans (GEBCO), Global Ocean Physics Reanalysis (GLORYS), and ERA5-Heat. They all provide regular latitude-longitude gridded data with horizontal global coverage.

The GEBCO 2021 dataset [27] gives worldwide elevation information in meters on a 30 arc-second grid, equivalent to 930 m (near the equator), therefore very localized specificities will not be considered. The bathymetry profile is extracted perpendicular to the coastline, based on the simplifying assumption that the SWAC pipeline will be laid normal to the coast. However, this may not always be the case, as the actual alignment of the pipeline can vary because of technical or environmental constraints.

The GLORYS dataset [28] has a horizontal resolution of 1/12°, corresponding to a grid size of approximately 9.3 km (near the equator), with 50 standard depth levels. For the assessment of SWAC potential, a climatology spanning from 2000 to 2020 is computed. Moreover, the influence of ENSO on the temperature source will be estimated by calculating the DJF mean (December, January, February), separately for all El Niño and La Niña events during the 20-year period.

The ERA-5 Heat dataset [29] will be used to highlight locations where there is a need for air conditioning. The data has a horizontal resolution of 0.25°, approximately 28 km (near the equator), and a temporal coverage from January 1940 to near real time on an hourly timestep. It covers all the globe except Antarctica (90N-60S, 180W-180E) and has two main variables: the Mean Radiant Temperature (MRT), and the Universal Thermal Climate Index (UTCI). The MRT is considering direct, diffuse and reflected solar radiation (function of solar elevation angle), along with downwelling (from atmosphere) and upwelling (from ground) thermal radiation [29]. The UTCI is a biometeorology parameter describing human physiological response to its thermal environment by combining temperature, humidity, wind speed and thermal radiation [30].

Heat stress is defined according to the 10 thermal stress categories. Therefore, an hour featuring with an UTCI superior to 26 will be considered exposed to heat stress. A heat stress rate will be calculated for 2022, as the ratio between the number of hours of exposure to heat stress and the total number of hours in the year. Table 1 summarizes the datasets used, their respective resolutions and purpose.

Table 1
Input datasets for SWAC potential estimation.

| Datasets | Resolution | Purpose |
|------------------------------------------------|-------------------------------------------------------|-----------------------------------------------------------------------------------|
| General Bathymetric Chart of the Ocean (GEBCO) | 30 arcsec \approx 930 m Elevation level | Estimate a SWAC pipeline length for different depths for a coast location |
| Global Ocean Physics Reanalysis (GLORYS) | 1/12° \approx 9.3 km 50 standard vertical levels | Give a correspondence between depths and the seawater temperature source targeted |
| ERA5-HEAT | 1/4° \approx 28 km Surface level | Highlight areas where air conditioning is required for thermal comfort |

Pipeline length approximation model

In order to estimate the length of a SWAC drawing pipeline for a coastal location, the bathymetry and seawater temperatures datasets presented before will be combined as shown in Fig. 1. Polar regions have been excluded from the study (beyond $\pm 60^\circ$ latitude). Regarding the length of the SWAC drawing pipeline, it is possible to install a pipeline up to a maximum length of 10 km using well-established methodologies with controlled risks. Beyond that, installation methods would require significantly more expensive naval resources. The upper limit considered impossible is 30 km, except for very specific configurations. For example, 20 out of those 30 km would be located in shallow depths (less than 50 m), with only the last 10 km descending to greater depths. However, in such a scenario, there would be a thermal loss issue to consider. For these reasons, it was decided to limit the drawing point to a maximum distance of 15 km from the coastline.

After identifying the nearest drawing point within a 15 km radius around the selected coastline point, their respective depths are compared to verify the accessibility of this drawing point. If the seawater temperature point is deeper than the maximum depth in the bathymetry profile, then a SWAC installation is considered as not feasible for this

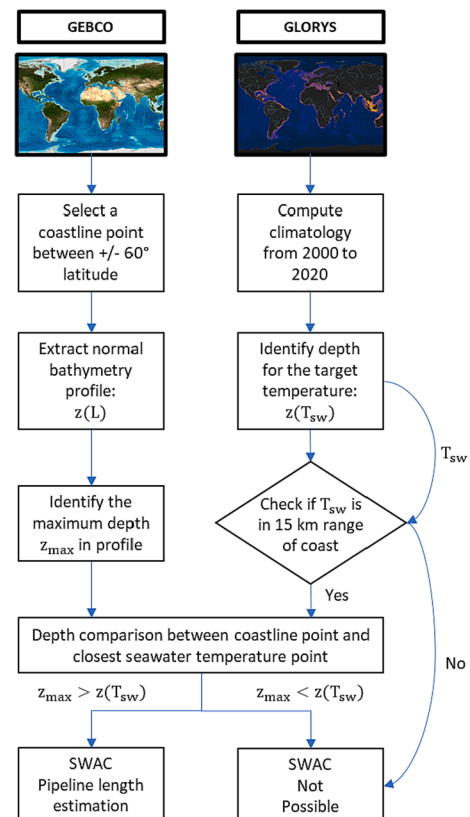


Fig. 1. Pipeline length approximation diagram.

location. Otherwise, the pipeline length is estimated based on the depth and the distance from the coast.

Cost analysis: Tahiti SWAC case

The total cost of the Tahiti SWAC project was \$ 34.7 million including taxes, and \$ 29.7 million excluding taxes. Costs are converted from euros based on the mean exchange rate for 2022 (EUR 1 = USD 1.12). This cost includes works on the District Cooling, which will not be considered as a cost for the SWAC installation. Therefore, the total cost for the SWAC alone is approximately \$ 26.9 million, excluding taxes, with the marine construction works accounting for around 75 % of this investment, amounting to \$ 20.3 million. A simplified cost analysis of SWAC can be done with the pipeline length as the single independent variable:

$$TC_{SWAC} = PC * L + FC \quad (1)$$

Fixed Costs (FC) include engineering studies, civil and process works, and other various costs, amounting to \$ 6.55 million. The Pipeline Cost (PC) corresponds to the approximated cost of one meter of installed pipeline, which is \$ 5359/m. This cost estimate is valid for pipeline lengths not exceeding 10 km due to the mentioned change in installation methods. However, this linear approach for pipeline cost is limited because the actual cost of a pipeline per meter tends to increase with longer pipeline lengths. Moreover, the pipeline diameter is not considered as a variable, despite its impact on the cost. Therefore, this Total Cost (TC) estimation becomes less precise with very different pipeline characteristics compared to the ones installed in Tahiti (3800 m length and 710 mm diameter). Cost data are summarized in [Table 2](#):

This simplified analysis could serve as a preliminary approximation of the savings obtained by changing the drawing point temperature from 5 °C to 12 °C.

Results and discussions

Global potential of SWAC systems

To assess the potential of the SWAC system, two world maps are presented. The first one, shown in [Fig. 2a](#), considers the conventional SWAC design with a 5 °C temperature intake, while the second map, in [Fig. 2b](#), depicts the alternative design with the higher temperature source of 12 °C. Both maps display the estimated lengths of intake pipelines, based on the five intervals defined as follows: 0 to 2.5 km in blue; 2.5 to 5 km in green; 5 to 7.5 km in yellow; 7.5 to 10 km in orange; 10 to 15 km in red.

Additionally, the heat stress rate for the year 2022 is depicted on the maps using a color bar. The heat stress rate corresponds to the proportion of hours throughout the year that exhibit heat stress according to the UTCL. This metric aims to highlight regions that are more likely to experience significant cooling needs throughout the year due to their climatic conditions. However, a lower heat stress rate does not necessarily indicate an irrelevant location for SWAC since, for instance, two deep-lake water air cooling installations exist in Canada and The Netherlands to supply the cooling needs during summer.

The dot color indicates the SWAC pipeline length, and the shading

Table 2
Cost data of Tahiti SWAC installation.

| Cost | Total | SWAC only (TC) | Pipeline (PC*L) | Pipeline meter (PC) | Fixed (FC) |
|----------------|-----------------|-----------------|-----------------|---------------------|-----------------|
| Taxes included | \$ 34.7 million | \$ 30.4 million | \$ 23.0 million | \$ 6056/m | \$ 7.40 million |
| Taxes excluded | \$ 29.7 million | \$ 26.9 million | \$ 20.3 million | \$ 5359/m | \$ 6.55 million |

represents the heat stress rate. The world map reveals that the most promising areas for SWAC technology are located in specific regions, mainly within the intertropical zone like the west coast of the USA, Mexico, Central American countries, the Caribbean, Hawaii, and French Polynesia. The eastern region like Japan, South Korea, Taiwan, and the Philippines also show potential for SWAC implementation. However, it is worth noting that there are relatively few highly favorable spots (blue dots) for the traditional SWAC configuration in those regions, with pipeline lengths generally around 5 km.

The areas favorable to SWAC have been intentionally represented independently of their current climate conditions. In a context of climate change, it is possible that some regions currently not experiencing thermal stress may face some in the future. By considering all areas, we acknowledge the potential shifts in climatic patterns and ensure that future possibilities are accounted for.

The new 12 °C temperature source for SWAC systems opens up opportunities to expand the technology to several new regions. These include countries such as Chile and Argentina in South America, Southern Africa, Oman in the Middle East, as well as some locations in Europe, such as Portugal, and the UK. Additionally, New Zealand also becomes a potential candidate for SWAC implementation. The two major regions of interest, North America, and Eastern Asia, that were previously identified for the 5 °C temperature source, remain significant. However, there is a noticeable difference in the estimated pipeline lengths, which are now shorter overall. It is worth highlighting that there are many spots with lengths in the range of 0 to 2.5 km, which were largely absent with the typical SWAC design. According to the two maps, the elevation of the drawing point significantly increases the number of eligible coastal points for SWAC (from 41,622 to 145,802) along the west and north-east coast of the United States and Mexico. The Caribbean region is eligible in both cases but experiences a significant reduction in pipeline length for the 12 °C case. In Eastern Asia, the maps demonstrate that a 12 °C intake temperature increases the number of coastal points available for SWAC (from 144,591 to 350,876), in southern Japan, western South Korea, Malaysia, Indonesia, and the Philippines. The 5 °C drawing point map shows almost no potential for the typical SWAC design in Europe except Finland and Sweden, whereas the 12 °C design expands the technology to south of UK, Ireland, Romania, Bulgaria, and few locations in North of Spain. The number of available locations in Europe changes from 14,995 to 56,819. The three areas of interest are detailed in individual maps available in [Supplementary materials](#).

The number of locations with the 5 °C and 12 °C source for each defined areas following the five intervals of [Fig. 2a](#) and [Fig. 2b](#) are summarized in [Table 3](#).

Besides the number of locations categorized by pipeline length for each selected areas and temperature, two additional indicators will be calculated to quantify the impact of this change of temperature source. The first indicator is the coastline point increase rate, which represents the proportion of additional points obtained with the drawing point change. This indicator measures the expansion of the eligible coastline for SWAC installations with the alternative design. The second indicator is the average length reduction, which quantifies the difference in pipeline length between the two SWAC configurations for the coastal points eligible in both cases. This indicator highlights the potential cost savings achieved by adopting the alternative design.

The region depicted on the map demonstrates an expansion of the number of coastal locations suitable for SWAC deployment by 350.3 %. Furthermore, the available coastal points, in either scenario, benefit from a significant reduction in pipeline length, with an average decrease of 4.0 km. This reduction translates into substantial cost savings, amounting to no less than \$ 21 million. The light green-colored points are expected to have installation costs similar to those of the Tahiti SWAC system.

In the same manner as done for the US region, the increase rate in favorable spots and the average reduction in length are calculated for

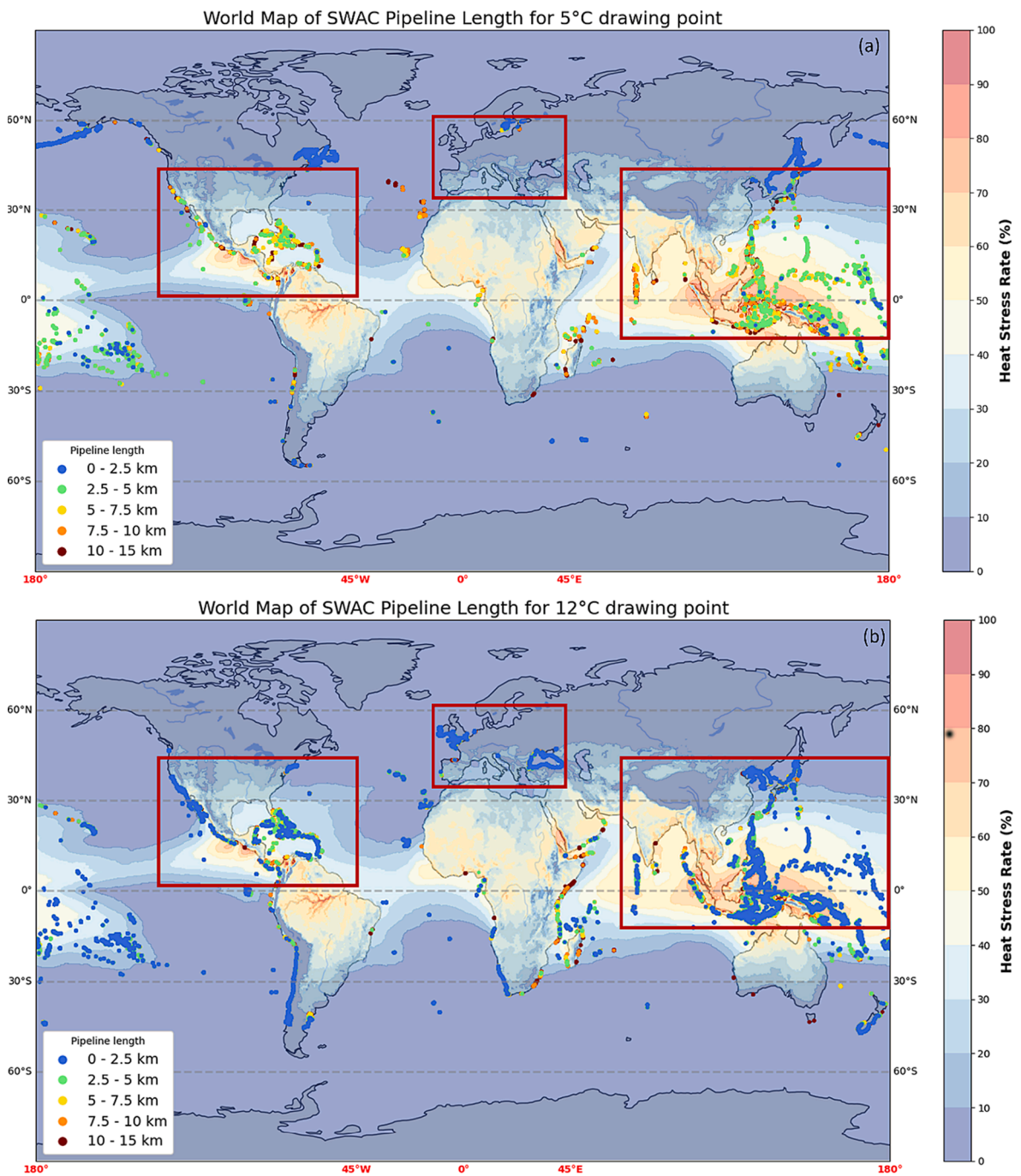


Fig. 2. Worldwide SWAC Potential for 5 °C (a) and 12 °C (b) temperature source. The red frames outline the areas of interest selected for the metrics calculations. (For interpretation of the references to color in this figure legend, the reader is referred to the web version of this article.)

Table 3
Number of locations categorized by areas and length for 5 °C and 12 °C water temperature source.

| For 5 °C/12 °C source | North America | Eastern Asia | Europe |
|-----------------------|------------------|-------------------|-----------------|
| 0 – 2.5 km | 418 / 38,884 | 13,319 / 94,489 | 5,627 / 37,729 |
| 2.5 – 5 km | 2,354 / 27,967 | 17,926 / 105,945 | 2,976 / 8,411 |
| 5 – 7.5 km | 9,830 / 30,676 | 40,951 / 56,688 | 2,914 / 5,583 |
| 7.5 – 10 km | 11,160 / 21,215 | 33,499 / 47,649 | 1,498 / 2,222 |
| 10 – 15 km | 17,860 / 27,060 | 38,896 / 46,105 | 1,980 / 2,874 |
| Total | 41,622 / 145,802 | 144,591 / 350,876 | 14,995 / 56,819 |

the Asian zone, which experiences a 242.7 % increase in the number of eligible coastal points for SWAC installations. Moreover, the available coastal points in either scenario show an average reduction of 4.4 km for the pipeline length. This reduction translates to cost savings of at least \$ 24 million.

The results of the aforementioned indicators, computed for the regions of North America, Eastern Asia and Europe are summarized in Table 4.

The viability of the SWAC project is strongly dependent on the cooling demand of the targeted location and its distance from the coastline. As the length of the pipeline approaches 10 km, equivalent to an estimated cost of around \$ 60.1 million, tax excluded, the cooling demand needs to be substantial (10 MW_{cool}) in order to justify the high

Table 4
Temperature source variation impact on SWAC potential based on coastline point increase rate and average length reduction.

| Areas | Coastline point increase rate | Average length reduction (Standard Deviation) | Drawing pipeline cost savings |
|---------------|-------------------------------|-----------------------------------------------|-------------------------------|
| North America | 350.3 % | 4.0 km ($\sigma = 2.3$ km) | \$ 21 million |
| Eastern Asia | 242.7 % | 4.4 km ($\sigma = 2.2$ km) | \$ 24 million |
| Europe | 378.9 % | No shared locations | No shared locations |

investment cost. For pipelines ranging from 10 to 15 km, the cost information from the Tahiti installation is insufficient to provide a satisfying approximation of the installation cost.

Impact of ENSO on the higher temperature source.

The impact of El Niño–Southern Oscillation (ENSO), first for El Niño and then for La Niña, are considered for the selected drawing point at 12 °C. According to Roemmich [22], significant temperature fluctuations within individual layers can obscure the smaller vertically averaged temperature change, where the ocean loses heat during periods of anomalously warm surface layers and gains heat when the surface layer is cool. While this effect is negligible for the deep depths of the typical SWAC system at a depth of 1000 m, it must be taken into consideration for the drawing point at 12 °C to ensure the reliability and performance of the system.

The temperature anomaly depicted represents the difference between the climatology and the DJF (December-January-February) average of El Niño or La Niña events during the climatology period. By analyzing the temperature anomalies, we can assess the deviation from the normal climate conditions during ENSO events and evaluate the

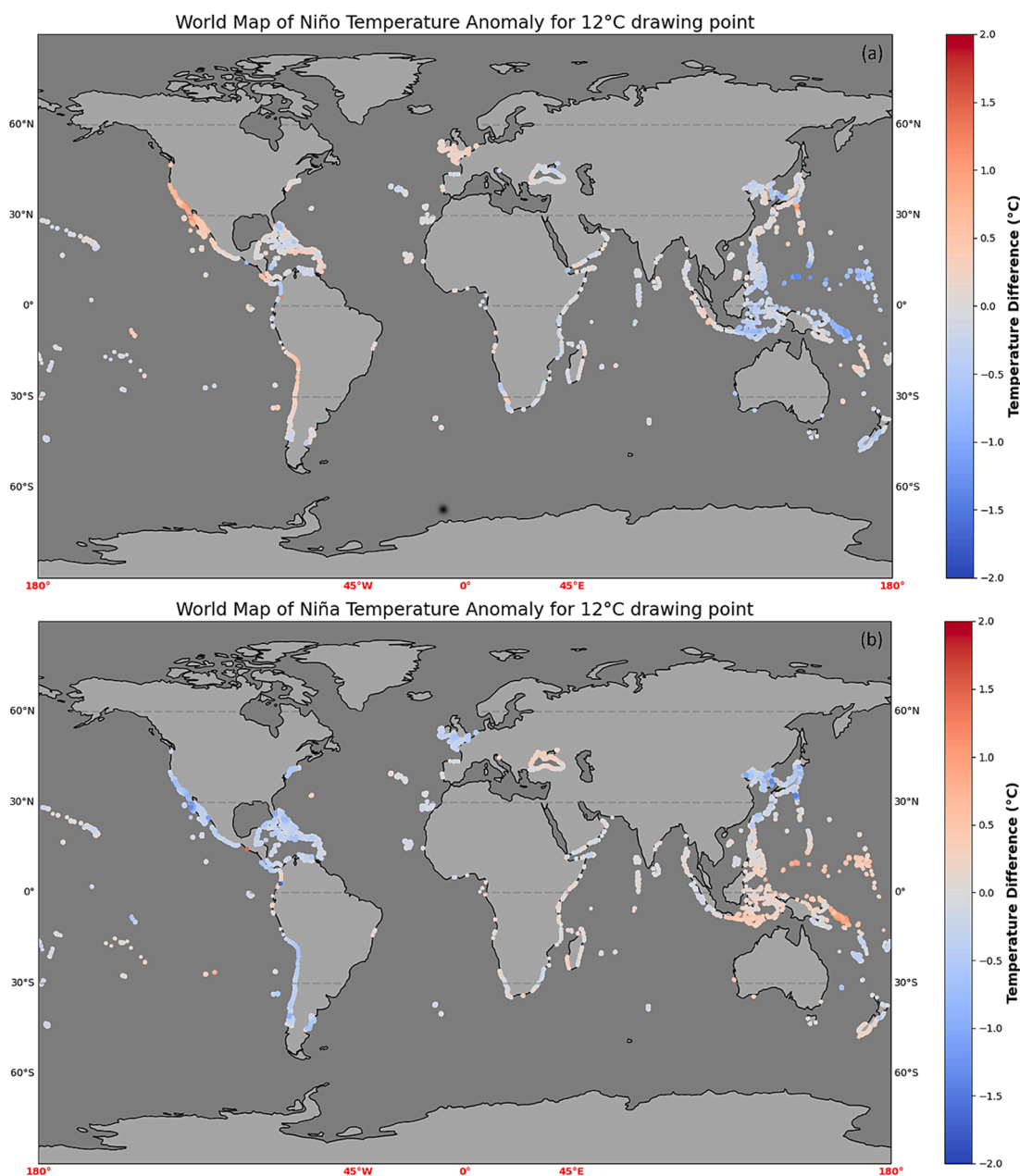


Fig. 3. El Niño (a) and La Niña (b) temperature anomaly for 12 °C isotherm.

potential effects on the selected drawing point.

The temperature source of 12 °C was chosen to match the temperature regime of HTDC (High Temperature District Cooling), which can operate with a temperature regime of 14/22 °C. According to the measurements on the Tetiaroa SWAC installation, heat loss along the primary pipeline results in an increase of approximately 1 °C at the heat exchanger inlet, added to 1 °C increase at the secondary outlet after the heat exchanger. Moreover, Jangsten [17] indicates that the supply temperature of the District Cooling can reach 16 °C or higher when dehumidification is managed by a separate ventilation system. Consequently, considering the impact of ENSO, the maximum allowable temperature anomaly tolerance for the drawing source during ENSO events is fixed between +1.5 °C and +2 °C.

The temperature anomalies at the depths of the previously selected drawing points are represented in Fig. 3a and Fig. 3b.

According to the map, the temperature variations generally remain within the range of half a degree Celsius (positive or negative), which is acceptable for SWAC operation. Only the west coast of North America (USA and Mexico) exhibits temperature variations of around 1 to 1.5 °C, and also a small area of islands in the south of Japan. The worldwide temperature variation extremes are −1.39 °C and +1.63 °C, which fall within the tolerable limits previously discussed and ensure the proper operation of the SWAC system during El Niño events.

Regarding La Niña events, the temperature variations extremes are of the same magnitude as El Niño, ranging from −1.41 °C to +1.72 °C. Additionally, the impact on temperature source variation on the selected spots remains acceptable, with deviations of 0.5 °C to 1 °C. The only exceptions concern a relatively small area in the south of Philippines and the east of Papua New Guinea, which experience temperature variations of about 1.5 °C. Overall, the effects of La Niña on the selected drawing point are within tolerable limits, ensuring the suitability and operational effectiveness of the SWAC system during La Niña events too.

In conclusion, ENSO has a relatively small influence on the temperature source selected for SWAC which does not prevent a proper operation of the SWAC system, despite the increase of the drawing point temperature. The impact of ENSO on the shallower drawing point of SWAC are summarized in the Table 5.

The stability of this temperature source, with its minimal variability and intermittency compared to other renewable energy sources, remains a strong advantage of the SWAC technology. Although, as mentioned in the introduction, dehumidification is most of the time ensured by the SWAC system alone. This could be, in certain cases, necessary to resort to an auxiliary device to reduce the relative humidity of the air. Consequently, with proper consideration and implementation of a suitable dehumidification solution, the SWAC system can continue to operate effectively, providing cooling efficiently and sustainably.

Conclusions

The study analyzes the potential of a Sea Water Air Conditioning (SWAC) system with two different drawing temperatures: 5 °C and 12 °C. The study assesses the global potential of SWAC by estimating pipeline lengths required to access the selected drawing point from coastlines worldwide. The results are depicted on world maps, showing the estimated pipeline lengths for different regions.

The favorable areas for SWAC with a 5 °C drawing temperature are mainly within the intertropical zone, such as the west coast of the USA, Mexico, Central American countries, the Caribbean, Hawaii, Taiwan, French Polynesia, Malaysia, Indonesia, and the Philippines. Japan and South Korea also show great potential. With the alternative 12 °C drawing temperature, the potential for SWAC expands to new regions, including Chile, Argentina, south of Africa, Oman, Portugal, the UK, and New Zealand.

Three main areas of interest are selected: North America, Eastern Asia, and Europe. The total number of eligible locations increases with the new drawing temperature, changing respectively from 41,622 to

Table 5

ENSO impact on SWAC temperature source.

| ENSO | Minimum | Maximum | Zone |
|---------|----------|---------|------------------------------------------------|
| El Niño | −1.39 °C | 1.63 °C | West coast of North America (USA, Mexico) |
| La Niña | −1.41 °C | 1.72 °C | East of Papua New Guinea, South of Philippines |

145,802, 144,591 to 350,876, and from 14,995 to 56,819. The study quantifies the impact of the temperature source change by calculating two indicators: the coastline point increase rate and the average length reduction. These indicators demonstrate the expansion of eligible coastal points for SWAC, and the cost savings achieved by adopting the alternative design. The North American zone demonstrates a coastline point increase rate of 350.3 %, with an average length reduction of 4.0 km and therefore a cost savings of \$ 21 million. The Eastern Asia area experiences a coastline point increase rate of 242.7 %, with an average length reduction of 4.4 km and therefore a cost savings of \$ 24 million. Europe has an increase rate of 378.9 % and, length reduction cannot be computed for this zone because of the absence of shared points.

The influence of El Niño–Southern Oscillation (ENSO) events is considered for the 12 °C drawing point. The results show that the temperature variations during ENSO events generally remain within acceptable limits for SWAC operation, with extremes temperature variations of 1.63 °C for El Niño and 1.72 for La Niña, both falling within tolerable ranges.

Overall, the study highlights the potential of SWAC technology in various regions worldwide, with the alternative 12 °C temperature source opening up opportunities in new areas. The shorter pipeline lengths associated with the 12 °C temperature source can lead to significant cost savings. Furthermore, the great stability of the temperature source remains a key advantage of SWAC technology, even with a higher drawing point. It is important to point out that the presented work only considers the current climate conditions. However, further work should explore the impact of future climate on the SWAC potential for two aspects. Firstly, in a context of climate change, certain regions are expected to be more exposed to thermal stress compared to the present climate, allowing SWAC technology to be relevant in more areas. Secondly, the intensifying ENSO events may have a more significant impact on the chosen drawing temperature.

CRediT authorship contribution statement

Kanhan Sanjiv: Conceptualization, Methodology, Software, Formal analysis, Investigation, Data curation, Writing – original draft, Visualization, Supervision. **Marania Hopuare:** Conceptualization, Software, Formal analysis, Investigation, Resources. **Anthony Jamelot:** Software, Formal analysis, Investigation, Resources, Data curation. **Franco Ferrucci:** Validation, Investigation, Writing – original draft, Writing – review & editing. **Olivier Marc:** Writing – review & editing, Project administration, Funding acquisition. **Franck Lucas:** Writing – review & editing, Project administration, Funding acquisition.

Declaration of competing interest

The authors declare that they have no known competing financial interests or personal relationships that could have appeared to influence the work reported in this paper.

Data availability

Data will be made available on request.

Acknowledgments

This work was supported by the French Environment and Energy

Management Agency (ADEME) and the University of French Polynesia. This study has been conducted using E.U. Copernicus Marine Service Information; 10.48670/moi-00021. The authors would like to thank Paul-Emmanuel Edeline for his valuable insights and feedback on data processing and visualization. Acknowledgements to David Wary for his advice on the conceptualization of the work and Alice Mounier-Vehier for her review as a native English speaker.

Appendix A. Supplementary data

Supplementary data to this article can be found online at <https://doi.org/10.1016/j.seta.2023.103601>.

References

- [1] Masson-Delmotte V, Pörtner H-O, Skea J, Zhai P, Roberts D, Shukla PR, et al. An IPCC Special Report on the impacts of global warming of 1.5°C above pre-industrial levels and related global greenhouse gas emission pathways, in the context of strengthening the global response to the threat of climate change, sustainable development, and efforts to eradicate poverty n.d.
- [2] International Energy Agency (IEA). The Future of Cooling. 2018.
- [3] Transition to sustainable buildings. strategies and opportunities to 2050. Paris: IEA Publ; 2013.
- [4] International Energy Agency (IEA). Cooling Emissions and Policy Synthesis Report. 2020.
- [5] Sanjiv K, Marc O, Davies N, Lucas F. Energy performance assessment of sea water air conditioning (SWAC) as a solution toward net zero carbon emissions: a case study in french polynesia. *Energy Rep* 2023;9:437–46. <https://doi.org/10.1016/j.egy.2022.11.201>.
- [6] Osorio AF, Arias-Gaviria J, Devis-Morales A, Acevedo D, Velasquez HI, Arango-Aramburo S. Beyond electricity: the potential of ocean thermal energy and ocean technology ecoparks in small tropical islands. *Energy Policy* 2016;98:713–24. <https://doi.org/10.1016/j.enpol.2016.05.008>.
- [7] ENGIE, RATP. Fraîcheur de Paris 2022. <https://www.fraicheurdeparis.fr/> (accessed October 14, 2023).
- [8] ENGIE. Thassalia : Inauguration de la première centrale française de géothermie marine 2016. <https://www.engie.com/journalistes/communiqués-de-presse/thassalia> (accessed October 14, 2023).
- [9] Herrera J, Sierra S, Ibeas A. Ocean thermal energy conversion and other uses of deep sea water: a review. *J Marine Sci Eng* 2021;9:356. <https://doi.org/10.3390/jmse9040356>.
- [10] Makai Ocean Engineering. Inc. OTEC: Ocean Thermal Energy Conversion; 2015. <https://www.makai.com/renewable-energy/otec/> (accessed October 14, 2023).
- [11] Lewis L, Trimble L, Bowers J. Open-cycle OTEC seawater experiments in Hawaii. *OCEANS '87* 1987:397–403. <https://doi.org/10.1109/OCEANS.1987.1160757>.
- [12] Okinawa Prefecture Department of Labor Commerce and Industry. Okinawa OTEC Demonstration Facility 2023. <http://otecokinawa.com/en/> (accessed October 14, 2023).
- [13] Kamogawa H. OTEC research in Japan. *Energy* 1980;5:481–92. [https://doi.org/10.1016/0360-5442\(80\)90072-9](https://doi.org/10.1016/0360-5442(80)90072-9).
- [14] Korea Research Institute of Ships & Ocean Engineering (KRISO), Korea Institute of Ocean Science and Technology (KIOST). 20kW OTEC pilot plant public demonstration in South Korea 2014. <http://otecnews.org/regional/pacific/20kw-otec-pilot-plant-public-demonstration-south-korea/> (accessed July 9, 2021).
- [15] Lee H-S, Lee S-W, Kim H-J, Jung Y-K. Performance characteristics of 20kW ocean thermal energy conversion pilot plant. *Am Soc Mech Eng Digital Collection* 2015. <https://doi.org/10.1115/ES2015-49768>.
- [16] ASHRAE. ANSI/ASHRAE Standard 55–2020. Thermal Environmental Conditions for Human Occupancy. Atlanta: ASHRAE; 2020. p. 2020.
- [17] Jangsten M, Filipsson P, Lindholm T, Dalenbäck J-O. High temperature district cooling: challenges and possibilities based on an existing district cooling system and its connected buildings. *Energy* 2020;199:117407. <https://doi.org/10.1016/j.energy.2020.117407>.
- [18] Boulinguez M, Fouquier A, Marc O, Castaing-Lasvignottes J. Cartographie des modèles de confort: application aux bâtiments en rafraîchissement mixte en climat tropical, 2022, p. 1.
- [19] Comparer deux régimes de température d'eau glacée pour un ventilateur-convecteur. *Energie Plus Le Site* 2007. <https://energieplus-lesite.be/evaluer/climatisation/5/comparer-deux-regimes-de-temperature-d-eau-glacee-pour-un-ventilo-convecteur/> (accessed October 22, 2023).
- [20] Marc O, Lucas F, Sinama F, Monceyron E. Experimental investigation of a solar cooling absorption system operating without any backup system under tropical climate. *Energy Buildings* 2010;42:774–82. <https://doi.org/10.1016/j.enbuild.2009.12.006>.
- [21] Praene JP, Marc O, Lucas F, Miranville F. Simulation and experimental investigation of solar absorption cooling system in Reunion Island. *Appl Energy* 2011;88:831–9. <https://doi.org/10.1016/j.apenergy.2010.09.016>.
- [22] Roemmich D, Gilson J. The global ocean imprint of ENSO. *Geophys Res Lett* 2011;38:n/a-n/a. 10.1029/2011GL047992.
- [23] Wen C, Kumar A, Xue Y, McPhaden MJ. Changes in Tropical Pacific Thermocline Depth and Their Relationship to ENSO after 1999. *J Clim* 2014;27:7230–49. <https://doi.org/10.1175/JCLI-D-13-00518.1>.
- [24] Xu K, Zhu C, He J. Linkage between the dominant modes in Pacific subsurface ocean temperature and the two type ENSO events. *Chin Sci Bull* 2012;57:3491–6. <https://doi.org/10.1007/s11434-012-5173-4>.
- [25] Yang G, Liu L, Zhao X, Li Y, Duan Y, Liu B, et al. Impacts of Different Types of ENSO Events on Thermocline Variability in the Southern Tropical Indian Ocean. *Geophys Res Lett* 2019;46:6775–85. <https://doi.org/10.1029/2019GL082818>.
- [26] Hunt JD, Byers E, Sánchez AS. Technical potential and cost estimates for seawater air conditioning. *Energy* 2019;166:979–88. <https://doi.org/10.1016/j.energy.2018.10.146>.
- [27] GEBCO Bathymetric Compilation Group. The GEBCO_2021 Grid - a continuous terrain model of the global oceans and land 2021. 10.5285/c6612cbe-50b3-0cfe-0553-6c86abc098f.
- [28] E.U. Copernicus Marine Service Information. Global Ocean Physics Reanalysis n.d. 10.48670/moi-00021.
- [29] Di Napoli C, Barnard C, Prudhomme C, Cloke HL, Pappenberger F. ERA5-HEAT: A global gridded historical dataset of human thermal comfort indices from climate reanalysis. *Geosci Data J* 2021;8:2–10. <https://doi.org/10.1002/gdj3.102>.
- [30] Bröde P, Fiala D, Błażejczyk K, Holmér I, Jendritzky G, Kampmann B, et al. Deriving the operational procedure for the Universal Thermal Climate Index (UTCI). *Int J Biometeorol* 2012;56:481–94. <https://doi.org/10.1007/s00484-011-0454-1>.